GSC Advanced Research and Reviews
eISSN: 2582-4597 CODEN (USA): GARRC2
Cross Ref DOI: 10.30574/gscarr
Journal homepage: https://gsconlinepress.com/journals/gscarr/

(RESEARCH ARTICLE)

Check for updates

Study of the chemical characterization and pore distribution of activated carbons synthesized from local agri-food waste (Niger)

Ousmaila SANDA MAMANE [1, 2], Rabilou SOULEY MOUSSA [2], Mahamane Nassirou AMADOU KIARI [2, 3, 4, *], Maman Hamissou IBRAHIM GREMA [3, 4], Ali SANDA BAWA [1, 2], Ousmane MAHAMAN SANI [1, 2], Maman Mousbahou MALAM ALMA [2] and Ibrahim NATATOU [1, 2]

[1] *National School of Engineering and Energy Sciences, University of Agadez, Niger.*
[2] *Department of Chemistry, Faculty of Science and Technology, Materials/ Water and Environment Laboratory/ Abdou Moumouni University, Niger.*
[3] *Laboratory of Industrial Processes of Synthesis, the Environment and New Energies (LAPISEN), Institut National Polytechnique Félix Houphouët-Boigny, BP 1093, Yamoussoukro, Côte d'Ivoire.*
[4] *African Centre of Excellence for the Recovery of Waste into High Value-Added Products (CEA-VALOPRO), Yamoussoukro, Côte d'Ivoire.*

GSC Advanced Research and Reviews, 2025, 24(03), 028–044

Publication history: Received on 26 July 2025; revised on 03 September 2025; accepted on 05 September 2025

Article DOI: https://doi.org/10.30574/gscarr.2025.24.3.0263

Abstract

The objective of this study is the chemical characterization and pore distribution of activated carbons (ACs) synthesized from local agri-food waste (Niger) by chemical means. The selected waste materials are the shells of *Balanites aegyptiaca* (BA) (L.) Del. and *Hyphaene thebaica* (HT) (L.) Mart. Orthophosphoric acid (H_3PO_4) and sulfuric acid (H_2SO_4) are used as impregnation agents. Next, the mass yields of ACs after pyrolysis, iodine (I_2) adsorption capacities, and methylene blue (MB) adsorption capacities are determined on the one hand, and total pore volume, cumulative pore volume (BJH), microporous volume, and average BET and BJH pore diameters are determined. Analysis of the results shows that the selected agri-food waste is a good precursor for the production of high-quality AC; it has very high cellulose content (67.6857% and 57.0571% for BA and HT, respectively). The pyrolysis temperature, concentration of the activating agent, and nature of the biomass have very significant effects on the yield of synthesized ACs. Activated carbons prepared by H_3PO_4 activation developed the best adsorption capacities. The total pore volumes range from CA-HT-1 (0.306531 $cm^3\ g^{-1}$) < CA-HT-2 (0.507390 $cm^3\ g^{-1}$) < CA-C (0.529036 $cm^3\ g^{-1}$) < CA-BA-1 (0.677426 $cm^3\ g^{-1}$) < CA-BA-2 (0.889648 $cm^3\ g^{-1}$). The average pore diameters range from CA-HT-1 (16.9788 Å) < CA-BA-1 (17.3617 Å) < CA-HT-2 (17.6995 Å) < CA-C (22.3516 Å) < CA-BA-2 (22.5136 Å). The pore diameters are essentially mesopores.

Keywords: Agri-Food Waste; Activated Carbon; Characterization; Porous

1. Introduction

In recent years, adsorption has remained one of the most widely used techniques for removing organic pollutants due to its effectiveness, ease of implementation, and affordable investment cost [1, 2,3]. This method requires the selection of an adsorbent with good characteristics (high adsorption capacity, availability, low cost, etc.). Thus, microporous adsorbents are widely used in the extraction of chemical species in aqueous or gaseous phases due to their excellent adsorption capacity a capacity linked to their large specific surface area and the development of their porosity [4, 5, 6]. To this end, the use of activated carbons (ACs) as adsorbents is of interest in the treatment of industrial wastewater. This is justified by the large exchange surface area developed by this material [7]. To date, numerous studies have been conducted on the transformation of solid waste into porous materials, particularly activated carbon (AC) [8]. These

* Corresponding author: Mahamane Nassirou AMADOU KIARI

materials have always played a major role in both domestic and industrial activities. Indeed, AC is by far the most widely used porous material, consisting mainly of carbonaceous material with a porous structure. It is a structure generally obtained after a high-temperature carbonization stage of lignocellulosic biomass (carbon-rich raw materials such as wood, peat, coal, lignite, coconut shells, peach pits, etc.), which has a very large specific surface area that gives it a high adsorption capacity [9]. ACs with very high adsorption capacity are particularly useful in water purification [6, 10], sugar decolorization [4, 11], volatile solvent recovery [4, 12], dye fixation, gas treatment [4, 13, 14], and in the process of extracting precious metals (gold and silver) from leaching solutions [10]; gold particles or nanoparticles being adsorbed in the porous matrix of the AC. Despite the availability of biomass in the subregion, our countries continue to import activated carbon for various applications, particularly in ore processing [15,16]. That is why, in this study, activated carbons are synthesized from local lignocellulosic biomass, notably the shells of *Balanites aegyptiaca* (L.) Del. and *Hyphaene thebaica* (HT) (L.) Mart. kernels, using chemical methods in order to study their chemical characteristics and pore distributions. Niger has abundant supplies of this biomass, which constitutes agri-food waste that is difficult to biodegrade in tropical countries [17,18]. Furthermore, two (2) activating agents are used in this study: orthophosphoric acid (H_3PO_4) and sulfuric acid (H_2SO_4). Next, the mass yields of the ACs after pyrolysis, the iodine (I_2) adsorption capacities, and the methylene blue (MB) adsorption capacities are determined on the one hand, and the total pore volume, cumulative pore volume (Vp) (BJH), micropore volume, and average pore diameter (BET and BJH) are determined.

2. Materials and methods

2.1. Thermal decomposition of Balanites aegyptiaca (L.) Del. and Hyphaene thebaica (HT) (L.) Mart. shells

The composition and physical properties of biomass are parameters that influence the conversion of lignocellulosic biomass into activated carbon. Thermogravimetric analysis (TGA) and differential thermal analysis (DTA) were performed on the shells of *Balanites aegyptiaca* (L.) Del. and *Hyphaene thebaica* (L.) Mart. to determine the mass decomposition of these materials. They were determined using a brand thermogram (Lab: METTLER STARe SW 8.10).

Figure 1 shows the sample of *Balanites aegyptiaca* (L.) Del. shells after crushing and sieving.

Figure 1 Shells of *Balanites aegyptiaca* (L.) Del. after crushing and sieving

2.2. Synthesis of activated carbons

After conditioning the raw materials, the activated carbons are produced in three stages [4, 19]:

- impregnation of the biomass in solutions of the activating agent;

- pyrolysis of the impregnated biomass;
- purification of the product obtained.

In this work, two activating agents are used, namely orthophosphoric acid (H_3PO_4) and sulfuric acid (H_2SO_4).

To optimize the performance of activated carbons synthesized from *Hyphaene thebaica* (L.) Mart., the effects of certain activation and pyrolysis parameters were studied. Table 1 shows the effect of activation and pyrolysis parameters.

Table 1 Optimization parameters for the production of ACEs

Biomass	**Parameters**	
Hyphaene thebaica (L.) Mart.	Concentration of the activating agent (%)	10 20 30 40 50
	Pyrolysis temperature (°C)	300 400 500 600 700

The samples of activated carbon synthesized following this optimization are used to determine the mass yields after pyrolysis, the iodine (I_2) adsorption capacities, and the methylene blue (MB) adsorption capacities.

2.3. Activation of the biomass sample

En 250 mL beakers, 16 g of the pretreated raw material and 100 mL of the activating agent solution (H_3PO_4 and H_2SO_4) are mixed together. The mixture obtained is stirred for 15 hours on a magnetic stirrer (Figure 2) at atmospheric pressure and room temperature. The sample is then filtered on ashless filter paper using a Büchner funnel (Figure 3), washed with distilled water, and dried in an oven at 105°C for 24 hours.

Figure 2 Impregnation on magnetic stirrers

Figure 3 Filtering the sample on a Büchner funnel

2.3.1. Pyrolysis of impregnated biomass samples

The dry sample obtained after impregnation was placed in a programmable high-temperature muffle furnace (Figure 4). The furnace temperature was gradually increased to the pyrolysis temperature (450°C) at a heating rate of 2.5°C min^{-1}, with an isothermal plateau of 1 hour 30 minutes at the end of heating, representing the residence time in the furnace.

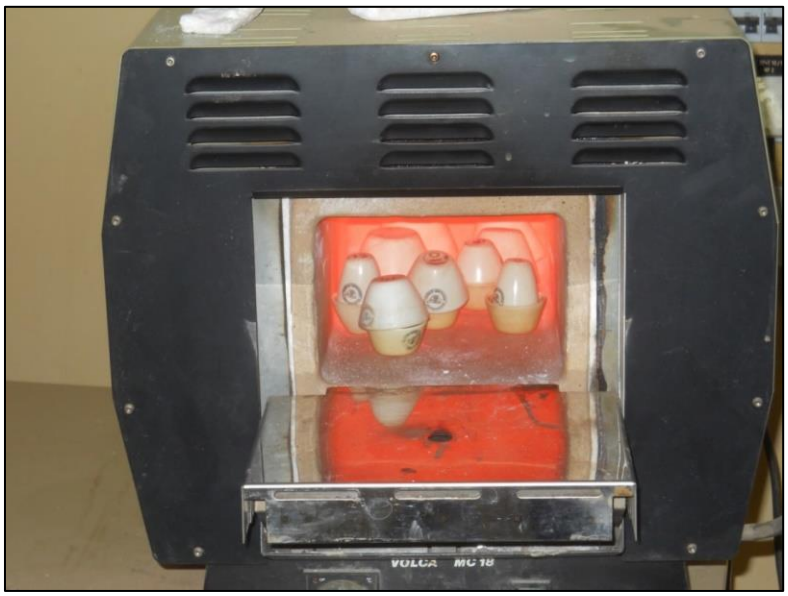

Figure 4 Muffle furnace

Upon removal from the furnace, the charred samples are cooled in a desiccator (Figure 5).

Figure 5 Cooling of samples in a desiccator

2.3.2. Purification

At the end of the production process, the cooled activated carbon is washed thoroughly with hot distilled water until the pH reaches between 6.5 and 7 to remove any impurities, then dried in an oven at 105°C for 24 hours. The processed activated carbon (PAC) is then cooled and stored in airtight containers until characterization tests are performed.

2.4. Chemical characterization of activated carbon

2.4.1. Yield calculation

The yield values for activated carbon production are determined using the following formula

$$\text{Yield (\%)} = \frac{\text{Mass}_{\text{final}}}{\text{Mass}_{\text{initial}}} \times 100 \qquad (1)$$

2.4.2. Determination of iodine adsorption capacities on synthesized activated carbons

The iodine index characterizes the areas accessible to any particle smaller than or equal to the size of the I_2 molecule, as well as their adsorption capacity, in particular the mini-micropores accessible to small particles responsible for tastes and odors. To determine iodine adsorption capacity, the procedure used by the Waste Study Center, which is an adaptation of the CEFIC 1989 method and AWWA B 600-78 standard, was used [4]. The experimental protocol is as follows: In a 100 mL beaker, 0.2 g of activated carbon powder (particle size less than 100 µm) was mixed with 20 mL of a 0.02 N I_2 solution. The mixture was stirred for 4 to 5 minutes and then filtered using a Büchner filter and ashless filter paper. Next, 10 mL of the filtrate was titrated with a 0.1 N $Na_2S_2O_3$ solution. Phenolphthalein was used as a color indicator. The iodine index Q_{I_2} is determined using the following formula (2) [5]

- Q_{I2}: adsorption capacity of I_2 or I_2 index (mg g^{-1});
- C_0: initial concentration of the I_2 solution (mol L^{-1});
- C_{thio}: concentration of $Na_2S_2O_3$ (mol L^{-1});
- V_{thio}: volume of $Na_2S_2O_3$ at equivalence (mL);
- V_{I_2}: volume of iodine titrated (mL);
- MI_2: molar mass of I_2 (g mol^{-1});
- V_{ads}: the adsorption volume (mL);
- m_{ca}: mass of activated carbon used (g).

$$Q_{I_2} = \frac{\left(C_0 - \frac{C_{thio}\, V_{thio}}{2V_{I_2}}\right) M_{I_2}\, V_{ads}}{m_{ca}} \qquad (2)$$

2.4.3. Determination of methylene blue (MB) adsorption capacities on synthesized activated carbons

The MB index, expressed in mg g^{-1}, represents the adsorption capacity of medium-sized molecules for the purpose of evaluating mesopores and macropores. MB adsorption was performed by introducing 0.1 g of CA, previously dried in an oven at 105°C, into a 250 mL Erlenmeyer flask containing 100 mL of the standard MB analysis solution. The mixture was stirred for 20 min. After this contact time, it was filtered through filter paper and the residual concentration of methylene blue in the solution was determined using a UV-visible spectrophotometer at a wavelength of 620 nm, which is the wavelength at which the adsorption of the MB molecule is maximum. Equation (3) gives the calculation of the Methylene Blue index.

$$Q_{BM} = \frac{(C_i - C_r)VM}{m_{ca}} \times 100 \quad (3)$$

- Q_{BM}: adsorption capacity of CA (in mg g^{-1});
- C_i: initial concentration of BM solution (in mol L^{-1});
- C_r: residual concentration of BM solution (in mol L^{-1});
- V: volume of the BM solution (in mL);
- M: molar mass of BM;
- m_{ca}: mass of CA used (in g).

2.5. Determination of the pore distributions of synthesized activated carbons

The porosities of four (4) samples of the Elaborated Activated Carbons (CA-BA-1; CA-BA-2; CA-HT-1 and CA-HT-2) and a Commercial Activated Carbon (CA-C) were determined. These analyses were carried out at the LABIRIS laboratory of the Université Libre de Bruxelles (ULB) in Belgium using a MICROMERITICS Gemini VII Surface Area and Porosity device by adsorption of liquid nitrogen N_2 at 77 K. The surface area occupied by a nitrogen molecule is equal to 0.162 nm^2.

The experimental protocol

A mass of 100 to 130 mg of the dry Activated Carbon sample was placed in a BET tube treated at 130°C, under a nitrogen flow, for 30 minutes using a MICROMERITICS FlowPrep 060 Sample Degas System. The sample was then allowed to return to room temperature, still under a nitrogen flow. The exact mass of the dry sample was determined to 1/10 mg just before connecting the tube to the BET measuring device.

Total pore volume

The total pore volume was determined using formula (4) at a point P/P0 = 0.99.

$$V_p = \frac{V_{ads}}{m_{CA}} \quad (4)$$

Vads is the amount of N2 adsorbed expressed in cm^3 and mCA is the mass of activated carbon in g.

The external volumes (mesopores + macropores) of CAEs and CA-C are determined from the total pore volumes minus the micropore volumes. Thus, the external specific surface areas are determined from the BET specific surface areas minus the micropore areas.

2.5.1. Cumulative pore volume (Vp) (BJH)

This is also determined by the Barret, Joyner, and Halenda (BJH) model (at adsorption and desorption) between 17,000 Å and 3,000,000 Å. It is obtained by plotting the cumulative pore volume curve (ΔVdesorbed) as a function of pore width (t). The pore volume is thus determined by the derivative of the curve.

2.5.2. Microporous volume

Total microporous volumes are determined at the initial partial pressure P/P^0 or using the t-curve method (Harkins and Jura). The latter is presented in this paper; it is obtained by plotting the curve of thickness (t) as a function of adsorbed volume. Thus, the linear regression line is plotted between 3.5 and 10 Å. The micropore volume was determined using the t-plot model and at the initial relative pressure. For the t-plot method, it is obtained by plotting the curve of the amount of N_2 adsorbed as a function of the statistical thickness t.

2.6. Average BET and BJH pore diameter

The average pore size was determined by the BET and BJH models (adsorption and desorption) using formula (5).

$$d_{moy} = \frac{4V}{S} \quad (5)$$

Where V is the amount of N_2 adsorbed expressed in $cm^3\ g^{-1}$ and S is the specific surface area in $m^2\ g^{-1}$.

3. Results

3.1. Characteristics of lignocellulosic biomass

Table 2 summarizes the results of immediate and thermal analyses performed on the shells of Balanites aegyptiaca (BA) (L.) Del. and Hyphaene thebaica (HT) (L.) Mart.

Table 2 Characteristics of lignocellulosic biomass used

Biomass	**Immediate analysis of biomass (%)**		
	Humidity rate	Ash content	Loss on ignition
Balanites aegyptiaca (L.) Del. *Hyphaene thebaica* (L.) Mart.	4.9914 5.0026	2.9994 5.8286	96.3619 98.9587
Biomasses	Biomass constituents(%)		
	Cellulose	Hemicellulose	Lignin
Balanites aegyptiaca (L.) Del. *Hyphaene thebaica* (L.) Mart.	67.6857 57.0571	5.9369 5.5598	26.3774 37.3831

3.2. Chemical Characterization of Activated Carbons

3.2.1. Mass yield after pyrolysis

The results of the mass yields of activated carbons produced by activation with H_3PO_4 are shown in Table 3.

Table 3 Mass yield after pyrolysis/H_3PO_4 activation

Biomass	**Parameters**		**Mass of CAE (g)**	**Yield (%)**
Hyphaène Thebeca	Concentration (%)	10	8.57	42.85
		20	8.29	41.45
		30	8.18	40.9
		40	9.41	47.05
		50	9.74	48.7
	Pyrolysis temperature (°C)	300	10.64	53.2
		400	6.7	33.5
		500	6.22	31.1
		600	6.26	31.3
		700	0.66	3.3

Table 4 shows the mass yield results for activated carbons produced by H_2SO_4 activation.

Table 4 Mass yield after pyrolysis/H_2SO_4 activation

Biomass	Parameters		Mass of CAE (g)	Yield (%)
Hyphaène Thebeca	Concentration (%)	10	7.38	36.9
		20	6.81	34.05
		30	6.59	32.95
		40	6.43	32.15
		50	5.18	25.9
	Pyrolysis temperature (°C)	300	8.82	44.1
		400	6.26	31.3
		500	2.82	14.1
		600	2.34	11.7
		700	3.42	17.1

3.3. Iodine adsorption capacities of synthesized activated carbons

The iodine indices of activated carbons produced by H_3PO_4 activation are shown in Table 5.

Table 5 Iodine adsorption capacity (mg g^{-1}) / H_3PO_4 activation

Biomass	Parameters		Volume of $Na_2S_2O_3$ at equivalence (mL)	Iodine adsorption capacity (mg g^{-1})
Hyphaène Thebeca	Concentration (%)	10	0.7	838.2
		20	0.4	914.4
		30	0.3	939.8
		40	0.1	990.6
		50	0.1	990.6
	Pyrolysis temperature (°C)	300	1.05	749.3
		400	0.4	914.4
		500	0.25	952.5
		600	0.9	787.4
		700	0.25	952.5

Table 6 shows the iodine index results for activated carbons produced by activation with H_2SO_4.

Table 6 Iodine adsorption capacity (mg g^{-1}) / H_2SO_4 activation

Biomasse	Parameters		Volume of $Na_2S_2O_3$ at equivalence (mL)	Iodine adsorption capacity (mg g^{-1})
Hyphaène Thebeca	Concentration (%)	10	0.9	787.4
		20	0.9	787.4
		30	0.9	787.4
		40	0.8	812.8
		50	0.7	838.2
	Pyrolysis temperature (°C)	300	2.4	406.4
		400	1.1	736.6
		500	0.8	812.8
		600	0.4	914.4
		700	0.3	939.8

3.3.1. BM index

The results of the BM indices for activated carbons produced by H3PO4 activation are summarized in Table 7.

Table 7 BM adsorption capacity (mg.100g^{-1}) /H_3PO_4 activation

Biomass	Parameters		Absorbance of residual solutions	BM adsorption capacity	Rate (%)
Hyphaène Thebeca	Concentration (%)	10	0.093666667	626.7051144	88.86115331
		20	0.092333333	627.8247305	89.01990481
		30	0.056333333	658.0543653	93.30619537
		40	0.028333333	681.5663035	96.63997691
		50	0.112333333	611.030489	86.63863228
	Pyrolysis temperature (°C)	300	0.023	686.044768	97.27498292
		400	0.012	695.2816008	98.58468281
		500	0.012333333	695.0016968	98.54499494
		600	0.037	674.2887989	95.60809215
		700	0.067333333	648.8175325	91.99649547

The results of the methylene blue indices of activated carbons produced by activation with H_2SO_4 are shown in Table 8.

Table 8 BM adsorption capacity (mg.100g^{-1}) /Activation

Biomass	Parameters		Absorbance of residual solutions	BM adsorption capacity	Extraction rate (%)
Hyphaène Thebeca	Concentration (%)	10	0.123333333	601.7936561	85.32893239
		20	0.082666667	635.9419473	90.1708532
		30	0.139333333	588.3582628	83.42391436
		40	0.048	665.051966	94.29839226
		50	0.103666667	618.3079936	87.67051704
	Pyrolysis temperature (°C)	300	0.187	548.3319871	77.74854816
		400	0.171666667	561.2075723	79.57419043
		500	0.077333333	640.4204117	90.80585921
		600	0.084333333	634.5424272	89.97241382
		700	0.067666667	648.5376285	91.9568076

3.3.2. Microporosity of CAEs and CA-C

Microporous volumes

The microporous volume corresponds to the volume determined at the origin of the line. The slope of the line gives the specific microporous surface area, i.e., S = Vads,liq/t. Figures 6, 7, 8, 9, and 10 show the t-curves for CAEs and CAC.

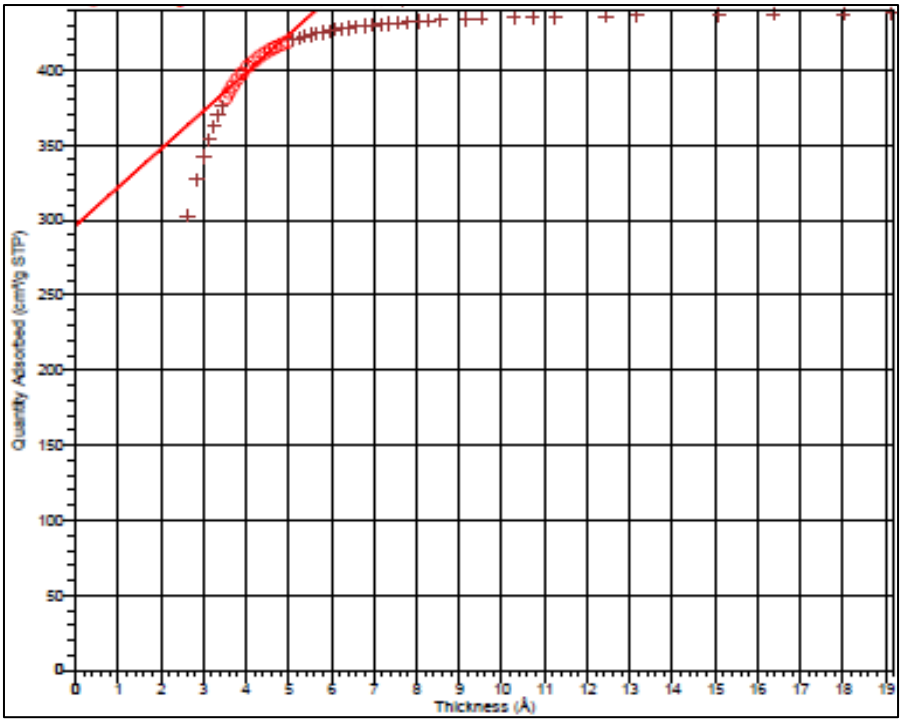

Figure 6 CA-BA-1 t-plot curve

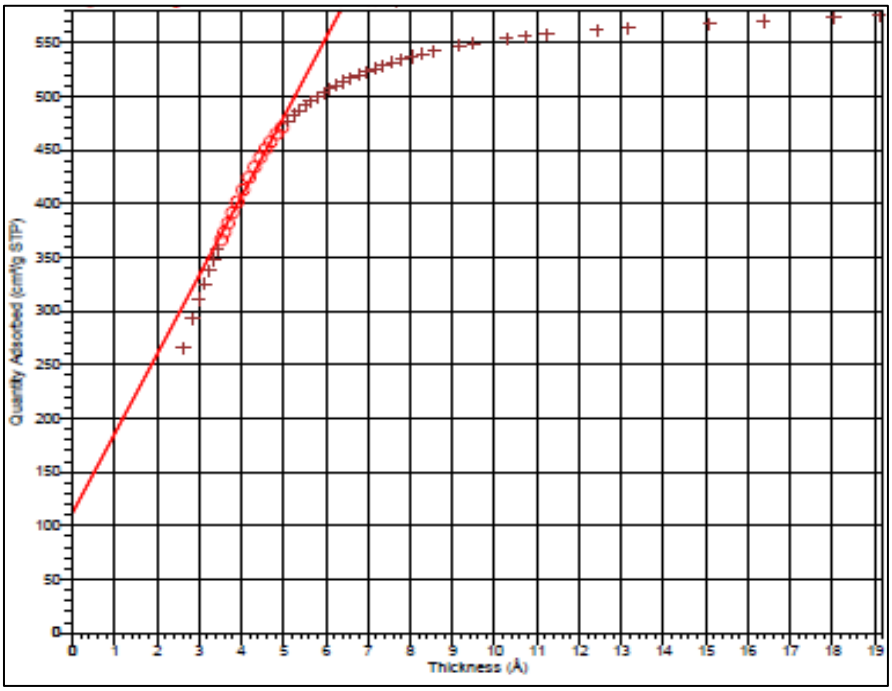

Figure 7 CA-BA-2 t-plot curve

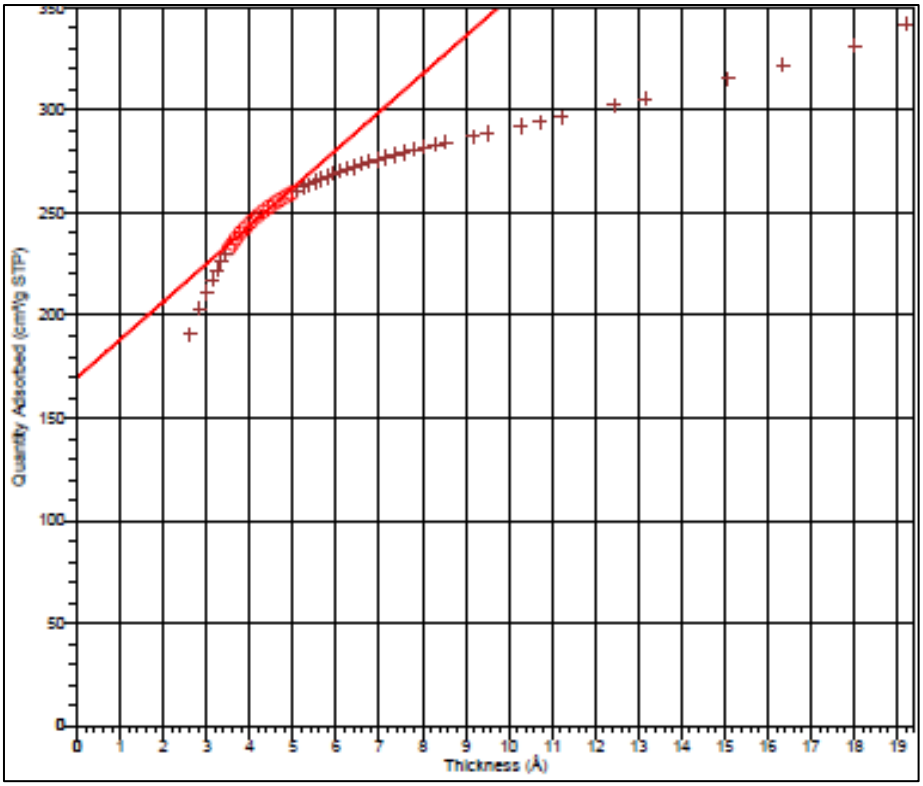

Figure 8 CA-C t-plot curve

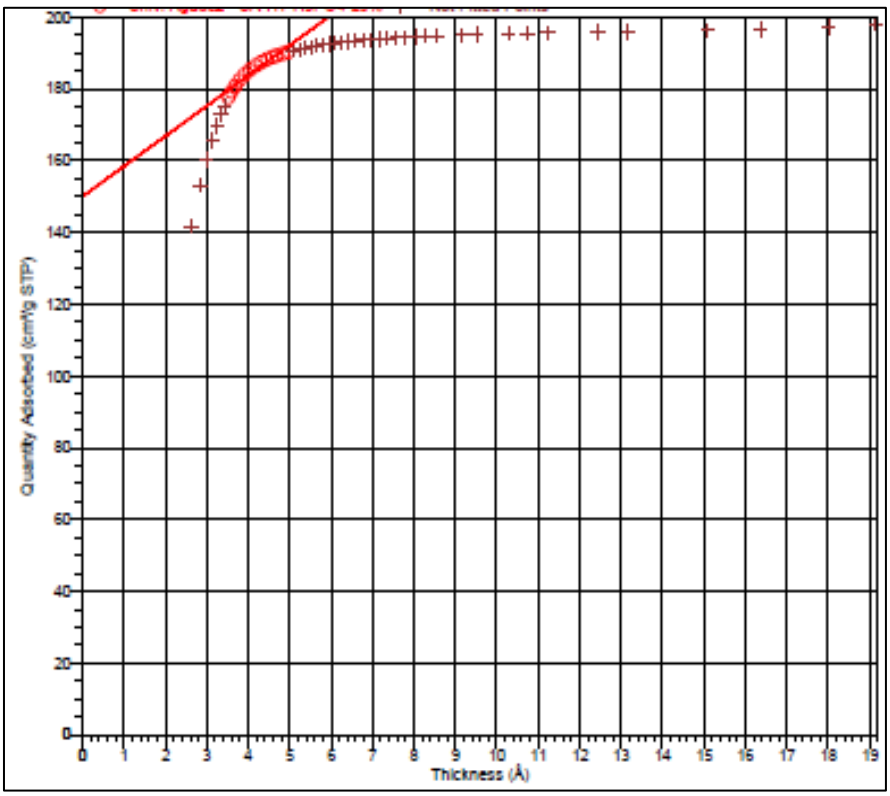

Figure 9 CA-HT-1 curve

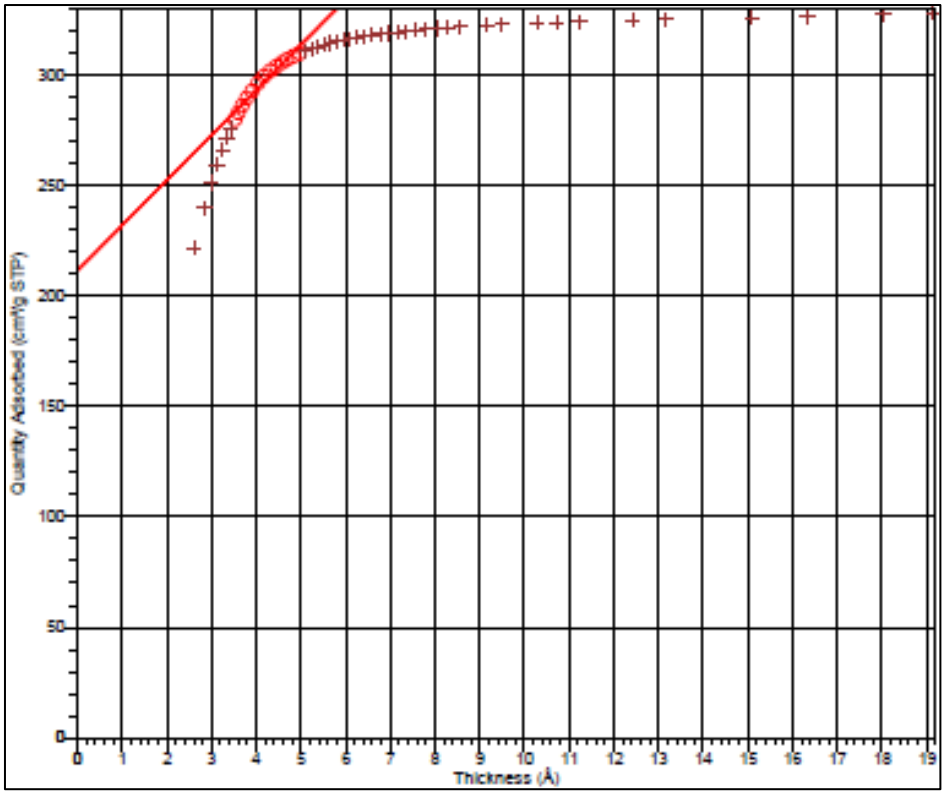

Figure 10 CA-HT-2 t-plot curve

All t-plot curves have a Z shape. This shape characterizes the existence of very small pores (micropores and mesopores) that fill at very low relative pressure through multilayer adsorption. This reduces the surface area available for subsequent adsorption.

Table 9 shows the results of the micropore volumes and specific micropore surfaces of the CAEs and CA-C.

Table 9 Micropore volumes of CAEs and CA-C

Ref. Samples	$V\mu_{pores}$ ($cm^3\ g^{-1}$ STP)	$S_{micropores}$ ($m^2\ g^{-1}$ STP)	R^2
CA-BA-1	0.458454	1167.4469	0.976459
CA-BA-2	0.173085	441.0802	0.994517
CA-C	0.262511	660.9931	0.989920
CA-HT-1	0.231967	591.7939	0.964626
CA-HT-2	0.327017	830.9311	0.978163

3.3.3. Total pore volumes

Total pore volumes are determined based on partial pressure $P/P^0 = 0.99$. Table 10 shows the results of this parameter on CAEs and CA-C.

Table 10 Total pore volumes

Ref. Samples	Voeux ($cm^3\ g^{-1}$ STP)
CA-BA-1	0.677426
CA-BA-2	0.889648
CA-C	0.529036
CA-HT-1	0.306531
CA-HT-2	0.507390

Mesopore and macropore volumes

The results for external volumes and surface areas are shown in Table 11.

Table 11 External volumes and surface areas of CAEs and CAC

Ref. Samples	Externes ($cm^3\ g^{-1}$ STP)	Externes ($m^2\ g^{-1}$ STP)
CA-BA-1	0.218972	393.2932
CA-BA-2	0.716563	1139.5578
CA-C	0.266525	285.7595
CA-HT-1	0.074564	130.3571
CA-HT-2	0.180373	315.7457

The external volumes (mesopores and macropores) were determined by subtracting the micropore volume from the total pore volume. They are approximately 0.074564; 0.180373; 0.218972; 0.266525; 0.716563 $cm^3\ g^{-1}$ for CA-HT-1, CA-HT-2, CA-BA-1, CA-C, and CA-BA-2, respectively. Thus, the SExt was determined (Table 11).

Table 12 shows the micropore volume and external volume ratios.

Table 12 Pore volume ratios

Ref. Samples	Porous volumes (%)	
	$\frac{V_\mu}{V_T}$	$\frac{V_{Ext}}{V_T}$
CA-BA-1	67.675879	32.324121
CA-BA-2	19.4554475	80.5445525
CA-C	49.6206307	50.3793693
CA-HT-1	75.674891	24.325109
CA-HT-2	64.4508169	35.5491831

4. Discussion

4.1. The results summarized in Table 2 show that

- the moisture content obtained is very low: 4.9914% and 5.0026% for *Balanites aegyptiaca* (L.) Del. (BA) and *Hyphaene thebaica* (L.) Mart. (HT) respectively. This could be an advantage for synthesizing ACs with high gross calorific value (GCV) [4];
- the ash content (2.9994% for BA and 5.8286% for HT) is relatively low. This would imply that the biomass consists mainly of organic matter. This parameter has a significant effect on the quality of ACs. The literature shows that a high ash content reduces the specific surface area and porosity of ACs. Indeed, the inorganic nature

of ash makes the activation process difficult because it clogs the pores of the carbon structure [20]. The values recorded during this work suggest that high-quality ACs can be produced;

- The loss on ignition values (volatile matter and fixed carbon) obtained from the samples are very high. They are 96.3619% for BA and 98.9587% for HT. Such values for volatile matter and fixed carbon are a good indicator for obtaining activated carbon with a high degree of graphitization, high calorific value, and a large number of functional groups [5];
- The biomasses have very high cellulose contents (67.6857% and 57.0571% for BA and HT, respectively). The presence of these cellulose contents is an advantage for obtaining ACs, especially through activation with H_3PO_4. The latter combines with glucose to form phosphate and polyphosphate bridges that connect and cross-link the biopolymer fragments. The insertion of phosphate groups leads to a swelling process which, after the acid is removed, leaves the matrix in a developed state with an accessible porous structure. The activation of cellulose produces a mixture of pore sizes. BA consists of more cellulose than HT; this suggests that CA derived from BA could have a larger specific surface area than that derived from HT;
- BA and HT nut shells have high lignin content (26.3774% and 37.3831% for BA and HT, respectively). This could be a good indicator for obtaining high pyrolysis yields, as lignin is the most thermally stable compound. Thus, HT should have a much higher mass yield after pyrolysis than BA;
- The nut shells of these biomasses are similar in hemicellulose content.

4.2. All these results suggest that BA and HT nut shells would be good precursors for CA production.

Analysis of the results presented in Tables 2 and 3 shows that the various tests carried out produced reproducible mass yields. These vary from 3.3 to 53.2%. The mass yield results obtained (Tables 2 and 3) show that the concentration and nature of the activating agent and the pyrolysis temperature are parameters that influence the mass yield. Thus, in both activation cases, the best yields are obtained at a pyrolysis temperature of 300°C: 53.2% in the case of H_3PO_4 activation (Table 2) and 44.1% when the activating agent is H_2SO_4 (Table 3). In general, the yield decreases as the temperature increases. In the case of H_3PO_4, the mass yield increases as the concentration of the activating agent increases. This is consistent with the results found by Siragi et *al.*, in 2017 [18] for the effect of orthophosphoric acid concentration. This could be explained by the fact that H_3PO_4 acid is an activating agent, thereby delaying the thermal decomposition of lignocellulosic biomass while limiting the loss of volatile matter, which would lead to the formation of a rigid carbon matrix [21]. In the case of activation by H_2SO_4, the yield decreases as the concentration increases. Overall, the yields of activated carbons prepared by activation with H_2SO_4 (Table 3) are low compared to those obtained by activation with H_3PO_4 (Table 2). Regardless of the activating agent considered, it can be seen that when the pyrolysis temperature is high, the yield decreases (Tables 2 and 3). Other authors [22] have made the same observations on ACs produced from sorghum grains by activation with H_3PO_4. They explained this by the fact that when the pyrolysis temperature is high, the biomass degrades to produce large quantities of volatile matter and a small quantity of activated carbon. This situation is a classic phenomenon in thermochemistry; when the heat and/or duration of exposure to the biomass increases, there is greater loss of macromolecules (cellulose, hemicellulose, and lignin) that make up the biomass.

The iodine index results compiled in Tables 4 and 5 range from 406.4 to 990.6 mg g^{-1}. These results show that the parameters studied have a real influence on iodine indices. The adsorption capacities of iodine increase as the concentration of the activating agent (H_3PO_4 and H_2SO_4) increases (Tables 4 and 5). Activated carbons prepared by H_3PO_4 activation developed the best iodine adsorption capacities compared to H_2SO_4 activation. Several authors have shown that the iodine index increases with the concentration of H_3PO_4, including Tchakala et al. in 2012 and Gueye [7,23]. These authors showed that the iodine index increases with the impregnation ratio. This was observed overall in their work. In the case of H_2SO_4 activation, the best iodine adsorption capacity (939.8 mg g^{-1}) is obtained at a pyrolysis temperature of 700 °C (Table 5). In both cases of activation, the increase in temperature significantly increases the I_2 adsorption capacities. These results confirm the work of Tchakala et *al.*, in 2012 [23]. The increase in temperature significantly promotes the development of micropores, leading to an increase in the adsorption capacity of activated carbons. Below 400°C, the pores are not well developed. Several studies in the literature have obtained similar results [24, 25, 26]. Cyrus A. et *al*., [25] noted an increase in the iodine index when the carbonization temperature was between 400 and 550°C. However, other research groups [27, 28] have noted that the iodine index increases significantly as the temperature rises. According to SILEX INTERNATIONAL's technical description of the quality criteria for activated carbon, the iodine index must be greater than 950 mg/g [29]. Many of the carbons produced by H_3PO_4 activation met this performance criterion. Therefore, they would have the ability to adsorb small molecules such as those responsible for tastes and odors [9]. These results are similar to those obtained by Siragi et *al*., in 2017 [16].

The results of the MB indices obtained for the different activated carbons in this study are summarized in Tables 6 and 7. They indicate the adsorption capacities and MB extraction rates. The results obtained show that the adsorption capacities of methylene blue vary from 548.3319871 to 695.2816008 mg.100 g^{-1} for H_2SO_4 and H_3PO_4. Activated carbons

prepared by activation with H_3PO_4 acid develop better BM adsorption capacities under the operating conditions used (Tables 6 and 7). In general, the BM adsorption capacity developed by activated carbons increases with the concentration of the activating agent and the pyrolysis temperature. The activated carbon with the best BM adsorption capacity was obtained with 25% H_3PO_4 and a pyrolysis temperature of 400°C. Similar results have been reported in the literature by Trachi et *al*., [30] on activated carbon obtained from bitter almond shells and by Gueye [4] on activated carbons obtained from olive pits. It has been reported that the methylene blue index is a parameter that can be used to evaluate mesopores (2 nm < diameter < 50 nm) and/or macropores (diameter > 50 nm) necessary for the adsorption of medium-sized molecules [31]. In the case of activation by H_2SO_4, the BM adsorption capacity values obtained are relatively low compared to those obtained by activation with H_3PO_4 (Tables 6 and 7).

4.3. The results presented in Table VIII show that

- the correlation coefficients (R^2) obtained are more or less significant. They are in the order of 0.976459; 0.994517; 0.989920; 0.964626 and 0.978163 respectively for CA-BA-1; CA-BA-2; CA-C; CA-HT-1 and CA-HT-2 (Table 8). This indicates that CA-HT-2 is better suited to this model than the others. They are then ranked as CA-C < CA-HT-2 < CA-BA-2 < CA-HT-1;
- The micropore volumes determined by the t-curve range from 0.173085 to 0.458454 $cm^3\ g^{-1}$ for CA-BA-2 and CA-BA-1, respectively. They range from CA-HT-1 (0.231967 $cm^3\ g^{-1}$) < CA-C (0.262511 $cm^3\ g^{-1}$) < CA-HT-2 (0.327017 $cm^3\ g^{-1}$). This shows that Vmicropores are proportional to Smicropores.
- The results presented in Table 9 show that the values of the total pore volumes of N_2-CAs (V_{poreux}) vary from 0.306531 to 0.889648 $cm^3\ g^{-1}$ for CA-HT-1 and CA-BA-2, respectively. This is consistent with the S_{BET} and S_L values. They are then ranked as follows for CA-HT-2 (0.507390 $cm^3\ g^{-1}$) < CA-C (0.529036 $cm^3\ g^{-1}$) < CA-BA-1 (0.677426 $cm^3\ g^{-1}$). This shows that the V_{poreux} of CA-C would be higher than that of CA-HT-2, whereas it should be lower given the S_{BET} developed by CA-HT-2. This could be explained by the phenomenon observed in the adsorption isotherms of these samples at P/P^0 =0.72628: At P/P^0 <0.72628, the volume of N_2 adsorbed by CA-C is lower than that of CA-HT-2. However, it becomes higher when P/P^0 >0.72628. The pore volume increases as the concentration increases. Mahamane Nassirou et *al*., [32] attempted to explain the activation process with H_3PO_4, proposing that H_3PO_4 reacts within the internal structure of cellulose to produce depolymerization, leading to an increase in pore volume (porous volume) and thus an expansion of the overall volume.

The $V\mu/V_T$ ratios are approximately 64.4508169, 67.675879, and 75.674891% for CA-HT-2, CA-BA-1, and CA-HT-1, respectively. These proportions exceed those of the V_{Ext}/V_T ratios obtained for these samples. This indicates the existence of a majority distribution of micropores compared to mesopores and macropores. This could be attributed to the essential distribution of type I adsorption isotherms. In the case of CA-C, the $V\mu/V_T$ and V_{Ext}/V_T ratios are similar (49.6206307 and 50.3793693%, respectively). This confirms the attribution of the adsorption isotherm to mixed type II (I + II). On the other hand, in the case of CA-BA-2, the distribution of mesopores and macropores is predominant (V_{Ext}/V_T = 80.5445525%). This also confirms the essential attribution of the adsorption isotherm to type II [33].

5. Conclusion

At the end of this study, we can draw the following conclusions

- The selected waste materials are good precursors for the production of high-quality charcoal; they consist almost entirely of highly carbonaceous organic matter;
- The waste has very high cellulose content (67.6857% and 57.0571% for BA and HT, respectively). The pyrolysis temperature, concentration of the activating agent, and nature of the biomass have very significant effects on the yield of synthesized ACs;
- Activated carbons prepared by H_3PO_4 activation developed the best iodine adsorption capacities compared to H_2SO_4 activation;
- Activated carbons prepared by H_3PO_4 acid activation develop better BM adsorption capacities under the operating conditions used;
- total pore volumes range from CA-HT-1 (0.306531 $cm^3\ g^{-1}$) < CA-HT-2 (0.507390 $cm^3\ g^{-1}$) < CA-C (0.529036 cm^3 g-1) < CA-BA-1 (0.677426 $cm^3\ g^{-1}$) < CA-BA-2 (0.889648 $cm^3\ g^{-1}$);
- external volumes are in the order of 0.074564; 0.180373; 0.218972; 0.266525; 0.716563 $cm^3\ g^{-1}$ for CA-HT-1, CA-HT-2, CA-BA-1, CA-C and CA-BA-2 respectively;
- micropore volumes range from CA-BA-2 (0.173085 cm^3 g-1) < CA-HT-1 (0.231967 $cm^3\ g^{-1}$) < CA-C (0.262511 $cm^3\ g^{-1}$) < CA-HT-2 (0.327017 $cm^3\ g^{-1}$) <CA-BA-1 (0.458454 $cm^3\ g^{-1}$);
- average pore diameters range from CA-HT-1 (16.9788 Å) < CA-BA-1 (17.3617 Å) < CA-HT-2 (17.6995 Å) < CA-C (22.3516 Å) < CA-BA-2 (22.5136 Å);

- CA-BA-1, CA-HT-1 and CA-HT-1 correspond to the micropore size distribution, while CA-C and CA-BA-2 correspond to the mesopore size distribution;
- access pore diameters (BJH desorption) range from CA-BA-2 (41.400 Å) < CA-BA-1 (42.400 Å) < CA-HT-2 (46.316 Å) < CA-HT-1 (52.964 Å) < CA-C (69.847 Å);
- actual pore diameters (adsorption) range from CA-HT-1 (20.525 Å) < CA-BA-1 (21.331 Å) < CA-HT-2 (21.537 Å) < CA-BA-2 (27.023 Å) < CA-C (37.995 Å);

pore diameters are predominantly mesoporous.

Compliance with ethical standards

Disclosure of conflict of interest

The authors declare no conflicts of interest regarding the publication of this paper.

References

[1] Ait Ahsene, Fetta, 2011, Magister, Adsorption du phénol par un mélange d'adsorbants (bentonite - charbon actif) 106 p.

[2] Ousmaila S M, Maâzou S.B. D, Abdoul Rachid C. Y, Maman Mousbahou M. A, Ibrahim N. Valorization of Balanites aegyptiaca (L.) Del. nut shells. and elimination of chromium in solution. Afrique SCIENCE, 14 (3), 2018, 167 – 181.

[3] Mahamane Nassirou Amadou Kiari, Affou Tindo Sylvie Konan, Ousmaila Sanda Mamane, Leygnima Yaya Ouattara, Maman Hamissou Ibrahim Grema,Maˆazou Siragi Dounounou Boukari, Abdourahamane Adamou Ibro, Maman Mousbahou Malam Alma, Kouassi Benjamin Yao. Adsorption kinetics, thermodynamics, modeling and optimization of bisphenol A on activated carbon based onHyphaene Thebaica shells. 2666-0164/© 2024 The Authors. Published by Elsevier Ltd. This is an open access article under the CC BY-NC-ND licenseN(http://creativecommons.org/licenses/bync-nd/4.0/). pp. 01 à 13 , 2024

[4] S. Zeroual et al, 2011, Revue, Estimation de l'hétérogénéité d'un charbon actif oxydé à différentes températures à partir de l'adsorption des molécules sondent. Energies Renouvelables ; vol.14 ; Nº 4 ; 581-590p.

[5] J. Avom et al, 2001, Revue, Adsorption Isotherme de l'Acide Acétique par charbons d'origine végétale, AJST. Science and Engineering series ; Vol.2 ; Nº2 ; 1-7p.

[6] Kheliel Oussama, 2014, Mémoire, Etude du pouvoir adsorbant du charbon actif pour la dénitrification des eaux souterraines. Génie civil et hydraulique ; Université Mohamed khider Biskra.

[7] Mbaye GUEYE, 2015, Thèse, Développement de charbon actif à partir de biomasses lignocellulosiques pour des applications dans le traitement de l'eau, Institut International de l'Ingénierie de l'Eau et l'Environnement (2iE) ; 215p.

[8] Drissa Bamba et al, 2009, Revue, Etudes comparées des méthodes de préparation du charbon actif, suivie d'un test de dépollution d'une eau contaminée au diuron, J. Soc. Ouest-Afr. Chim, 028, 41-52p.

[9] Nassim RIZOUG, 2006, Thèse, Modélisation électrique et énergétique des supercondensateurs et méthodes de caractérisation, Application au cyclage d'un module de supercondensateurs basse tension en grande puissance, Université des Sciences et Technologies de Lille, 201p

[10] Mohamed Zarrouki, 1990, thèse, Etude de l'Adsorption dans un Système Liquide-Solide: Solution d'Ion Dicyanoaurate-Charbon Actif', Ecole Nationale Supérieure des Mines de Saint-Etienne-France.

[11] Rabilou Souley Moussa, Ousmaila Sanda Mamane, Issa Habou, Maman Mousbahou Malam Alma and Ibrahim Natatou. Determination of the surfaces functions and of the pH at the point of zero charges of powdered activated carbons produced from the shells of the nucleus of Balanites aegyptiaca and Zizyphus mauritiana. World Journal of Advanced Research and Reviews Article DOI: https://doi.org/10.30574/wjarr.2022.16.3.143. pp. 893 à 904 . 2022

[12] W.H. Lee, P.J. Reucroft, Revue, Vapor Adsorption on Coal-and Wood-Based Chemically Activated Carbons (III) NH3 and H2S Adsorption in the Low Relative Pressure Range, Carbon, Vol. 37, N°1, pp. 21 - 26.

[13] C. Namasivayam, K. Kadirvelu, Revue, 1999, Uptake of Mercury (II) from Wastewater by Activated Carbon from an Unwanted Agricultural Solid By-Product: Coir-Pith, Carbon, Vol. 37, N°1, pp. 79 – 84.

[14] A. Houas, I. Bakir, M. Ksibi et E. Elaloui, 1999, Revue, Etude de l'Elimination du Bleu de Méthylène dans l'Eau par le Charbon Actif Commercial CECA 40, Journal de Chimie-Physique et de Physico-Chimie Biologique, Vol. 96, N°3, pp. 479 – 486.

[15] Siragi D. B M, Desmecht D, Hima H. I, Mamane O. S, Natatou I. Optimization of Activated Carbons Prepared from andlt;iandgt;Parinari macrophyllaandlt;/iandgt; Shells. MSA, vol.12, no 05, 2021, p. 207-222, doi: 10.4236/msa.2021.125014.

[16] Ousmaila S.M, Maˆazou S.D.B, Mousbahou M.A.M, Ibrahim N. Valorisation des coques de noyaux de Balanites aegyptiaca (L.) Del. et Hyphaene th´ebaica (L.) Mart, pour l'´elaboration et caracterisation de Charbons Actifs; application pour l'elimination du chrome. ESJ 14 (2018) 195, https://doi.org/10.19044/esj.2018.v14n21p195

[17] Ousmaila, S.M., Adamou, Z., Ibrahim, D., and Ibrahim, N. (2016). Préparation et caractérisation de charbons actifs à base de coques de noyaux de Balanites eagyptiaca et de Zizyphus mauritiana : J. Soc. Ouest-Afr. Chim. 041, 59-67.

[18] Maâzou, S.D.B., Hima, I. H., Maman Mousbahou, M. A., Adamou, Z., and Ibrahim, N. (2017). Elimination du chrome par du charbon actif élaboré et caractérisé à partir de la coque du noyau de Balanites agyptiaca : Int. J. Biol. Chem. Sci. 11 (6) 3050-3065. DOI : https://dx.doi.org/10.4314/ijbcs.v11i6.39.

[19] Barrow N. J. (1978). The description of phosphate adsorption curves : J. Soil Sci., 29 (4) 447-462. DOI : https://doi.org/10.1111/j.1365-2389.1978.tb00794.x

[20] Demirbas, A. (2004). Effect of initial moisture content on the yields of oily products from pyrolysis of biomass : J. of analytical and applied pyrolysis 2, 803-815

[21] Zhao, J., Lai, C., Dai, Y. and Xie, J. (2007). Pore structure control of mesoporous carbon as supercapacitor material : Materials Letters., 61, 4639-4642. DOI : https://doi.org/10.1016/j.matlet.2007.02.071

[22] Diao, Y., Walawender, W. P. and Fan, L.T. (2002). Activated carbons prepared from phosphoric acid activation of grain sorghum : Bioresource Technology, 81, 45-52. DOI : https://doi.org/10.1016/S0960-8524(01)00100-6

[23] Tchakala, I., Bawa, L. M., Djaneye-Boundjou, G., Doni, K.S., and Nambo, P. (2012). Optimisation du procédé de préparation des charbons actifs par voie chimique (H3PO4) à partir des tourteaux de Karité et des tourteaux de Coton : Int. J. Biol. Chem. Sci. 6 (1), 461–478. DOI : http://dx.doi.org/10.4314/ijbcs.v6i1.42

[24] Mohammad, A., Mohammad, A. R., Mohammad, A. M. and Mohammad, B. S. (2007). Adsorption Studies on Activated Carbon Derived from Steam Activation of Jute Stick Char : J. Surface Sci. Technol., 23 (1-2) 73-80.

[25] Cyrus, A., Tahereh, K., Seyed, M. L. and Mansooreh, S. (2006). Chemical Production of Activated Carbon from Nutshells and Date Stones : Chem. Eng. Technol., 29 (8) (2006) 986-991. DOI: https://doi.org/10.1002/ceat.200500325

[26] Monneyron, P., Faur-Brasquet, C., Sakoda, A., Suzuki, M. and Cloirec, P. (2002). Competitive Adsorption of Organic Micropollutants in the Aqueous Phase onto Activated Carbon Cloth: Comparison of the IAS Model and Neural Networks in Modeling Data : Langmuir, 18 (13) 5163-5169. DOI : https://doi.org/10.1021/la020023

[27] Girgis, B. S. and El-Hendawy, A. (2002). Porositydevelopment in activated carbons obtained from datepits under chemical activation with phosphoric acid : Microporous Mesoporous meter, 52, 105-117.

[28] Gratuito, M. K. B., Panyathanmaporn, T. Chumnanklang, R. A., Sirinuntawittaya, N. B. and Dutta, A. (2008). Production of activated carbon from coconut shell : Optimization using response surface methodology : Biosour. Technol., 99 (11) 4887-4895. DOI : https://doi.org/10.1016/j.biortech.2007.09.042

[29] Silex International. Charbon actif haute qualité, T2, Activ'OG8*30. www.silexinternational.com

[30] Trachi, M., Bourfis, N., Benamara, S. and Gougam, H. (2014). Préparation et caractérisation d'un charbon actif à partir de la coquille d'amande (Prunus amygdalus) amère : Biotechnol. Agron. Soc. Environ., 18 (4) 492-502.

[31] Julien, O. and Lydie, C. (2010). Evaluation de charbons actifs en poudre (CAP) pour l'élimination des micropolluants dans les eaux résiduaires urbaines. Ecole Polytechnique Fédérale de LAUSANNE EPFL, Lausanne-Suisse LS, 62.

[32] AMADOU KIARI Mahamane Nassirou, KONAN Affoué Tindo Sylvie, SANDA MAMANE Ousmaila, KONE Horo, FANOU Guy Didier, SIRAGI DOUNOUNOU BOUKARI Maâzou, IBRAHIM GREMA Maman Hamissou, MALAM ALMA Maman Mousbaou, YAO Kouassi Benjamin. Influence of Orthophosphoric Acid Activation on the Quality of Activated Carbons. Materials Science Forum Submitted: 2023-02-04 ; ISSN: 1662-9752, Vol. 1122, pp 91-98 Accepted: 2023-07-26 © 2024 Trans Tech Publications Ltd, Switzerland. pp. 91 à 98, 2024

[33] Ousmaila, SM. Valorization of agro-food wastes for the elaboration of activated carbons; characterization and application in the depollution of wastewater loaded with chromium from the Malam Yaro Tannery of Zinder-Niger. [Doctoral thesis]. Abdou Moumouni University of Niamey. These of Doctorate Chemistry of Metals ; 2019.